

THE PERFORMANCE OF THE DC MOTOR BY THE PID CONTROLLING PWM DC-DC BOOST CONVERTER

Erol CAN, Hasan Hüseyin SAYAN

Abstract: This paper presents the PID controlling direct current (DC) to the direct current boost converter feeds DC motor which has a 3.68 kW and 240 V of DC voltage input on its characteristics. What is first formed is the boost converter mathematical model at the design stage. Secondly, a mathematical model of the DC motor is created so that the boost converter with the machine can be established and modeled at the Matlab Simulink. The PID controller is considered for arranging a pulse width modulation for a boost converter switch because the needed voltage is provided for a DC motor. After that, the PID controlling direct current (DC) to a direct current boost converter running the DC motor is implemented at the Matlab Simulink. In addition to that, the only constant source running the DC motor is simulated at the Matlab Simulink. The DC motor operated by the PID controlling converter that has a low input voltage is compared to the DC motor operated by the high constant DC voltage. A low voltage input converter controlling the DC motor has a high performance according to the high constant DC source running the DC motor.

Keywords: DC-DC converter; DC motor; PID control; step-sinus pulse width modulation

1 INTRODUCTION

Many researchers deal with the speed control of the DC machine since DC motors are controlled over a wide range with stable and linear characteristics. DC motors are preferred at the industrial working areas because of the stable speed and load performance [1÷3]. In addition to that, sometimes dc energy on systems may be inadequate although direct voltage sources are needed for the operation of DC motors. The DC-DC converters are considered good selection for supplying the load when the direct current sources are not sufficient. So, the DC-DC converters are very important at the DC energy regulation, generation systems and power applications. Some control techniques have to be used for the increase performance of the power circuit using DC sources [4÷8]. The PID control techniques have been applied for the controlling of some power systems [9÷10]. In the study, the PID control using the step sinus pulse width modulation (SSPWM) DC-DC boost converter is unlike the similar studies [11÷13]. The DC-DC boost converter of the mathematical model for the system first part is designed so that the DC-DC boost converter can increase a low-level DC voltage (150 V) to a high-level value (520 V). After that, a mathematical model of the DC motor for the system second part is created to perform at the Matlab Simulink. For the regulation of the low DC voltage, the PID control is applied from the output speed of the DC motor to the switch of DC-DC converter after the converter is connected to the DC motor as in Fig. 1. The DC motor with the DC-DC boost converter, the DC motor with the constant DC source are modeled at the Matlab Simulink for the observation and the comparison of output performances, which are toques, rotor speeds, and currents. The DC-DC boost converter drives DC motor with 150 V on a closed-loop with the PID control, while the constant DC source runs the DC motor by 240 V on an open-loop which is

uncontrolled. The running DC motor with a DC-DC converter on a closed-loop control has the demanded results such as high settlement current and torques, even though the running DC motor with the constant DC source has high voltage on an open-loop control.

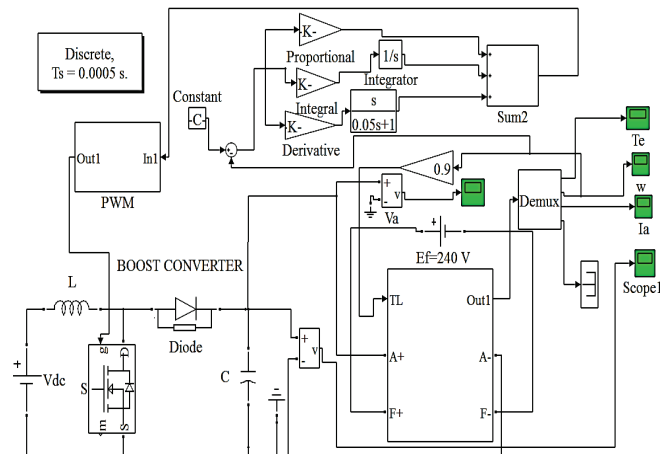


Figure 1 PID controlling the DC-DC boost converter running the DC motor

2 BOOST CONVERTER

Fig. 2 shows the power circuit which operates to raise a direct voltage. Firstly, the power circuit of the mathematical model is obtained by the relation between the input and output voltage equations when the MOSFET switch that is an active component is operating the passive components such as inductor, resistance and capacitor. In the equations, V_g is the value of input voltage, V_L is the value of inductance voltage, and i_L is the value of inductance current, R is the resistive load, C is the capacitor for converter output voltage, and D is the duty time for the switches.

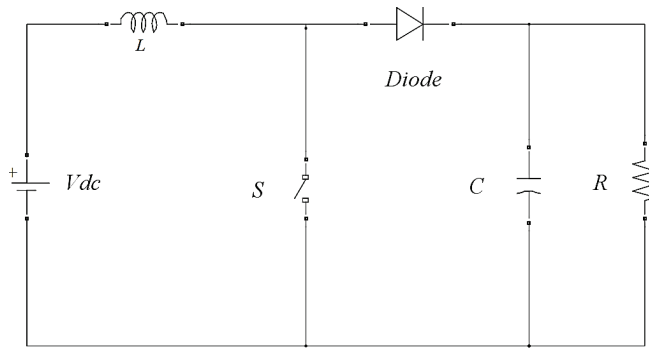


Figure 2 Boost converter circuit model

For the equation of state space, the form of equations and the relations between the current of inductance and the voltage of output have to be formed to a $\dot{x} = Ax + Bu$ form.

For $S = ON$

$$V_g = VL \tag{1}$$

$$\frac{di_L}{dt}L = V_g \tag{2}$$

$$i_L = \frac{V_g}{L} \tag{3}$$

$$\dot{V} = \frac{I_z}{C} \tag{4}$$

The variables obtained in the above shown equations are shown in the matrix form as follows.

$$\begin{bmatrix} \dot{i} \\ \dot{V} \end{bmatrix} = \begin{bmatrix} 0 & 0 \\ 0 & 0 \end{bmatrix} \begin{bmatrix} I \\ V \end{bmatrix} + \begin{bmatrix} \frac{D}{L} & 0 \\ 0 & \frac{D}{C} \end{bmatrix} \begin{bmatrix} V_g \\ I_z \end{bmatrix} \tag{5}$$

For $S = OFF$

$$V_g = VL + V_c \tag{6}$$

$$\frac{di_L}{dt}L = V_g - V_c \tag{7}$$

$$\frac{di_L}{dt} = \frac{V_g - V_c}{L} \tag{8}$$

$$i = \frac{V_g}{L} - \frac{V_c}{L} \tag{9}$$

$$\dot{V} = \left(I - \frac{V}{R} + I_z \right) \frac{1}{C} \tag{10}$$

$$\dot{V} = \frac{I}{C} - \frac{V}{RC} + I_z \frac{1}{C} \tag{11}$$

A and B matrix are calculated to form the state space which has the required variables for the boost converter. A as the given Eq. (12), and B as given Eq. (13).

$$A = DA_{on} + (1-D)A_{off} \tag{12}$$

$$B = DB_{on} + (1-D)B_{off} \tag{13}$$

Eqs. (14) and (15) show the matrixes on the final form:

$$A = (D-1) \begin{bmatrix} 0 & -\frac{1}{L} \\ -\frac{1}{C} & -\frac{1}{RC} \end{bmatrix} \tag{14}$$

$$B = \begin{bmatrix} \frac{D}{L} & 0 \\ 0 & \frac{1}{C} \end{bmatrix} \tag{15}$$

3 DESIGN OF THE PULSE WIDTH MODULATION

The pulse width modulation technique is widely considered for the motors drive and different loads drive at the some studies [15÷20]. The paper deals with the modulation technique. The technique is that the step-sinus pulse width modulation (SSPWM) showed in Fig. 3 controls the switch of the DC-DC converter. SSPWM is formed when two different triangles compare to the step sinus signals. The switching times can be determined with triangular similarity, because the steps of sinus signal increase the b unit lengths on the vertical and different the k unit lengths on the horizontal, as shown in Fig. 3. The creating voltage on loads is calculated as analytic because the interactions of steps with the triangles form similar triangles. Every formed triangle has a different size in all formed triangles. Pulse widths are produced because the similar triangle rules are shaped in the half period ($T/2$). Pulse widths are shown in Fig. 4 as similar triangles. D_f is the first pulse width, D_a is the average pulse width, and n is the pulse number.

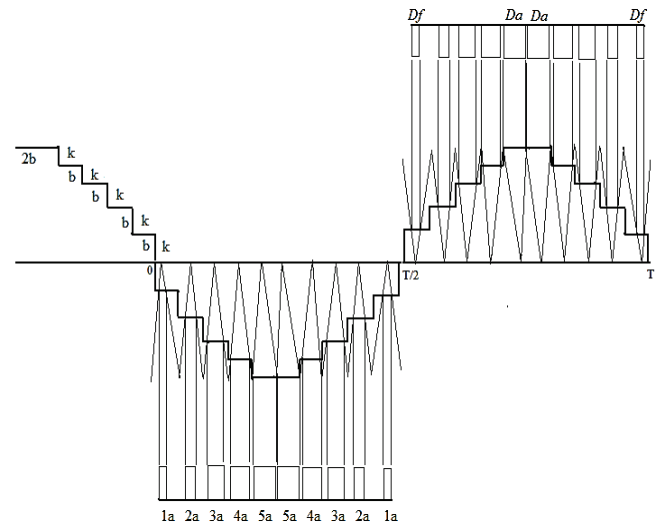


Figure 3 (a) Steps compared with the triangles, (b) formed triangles

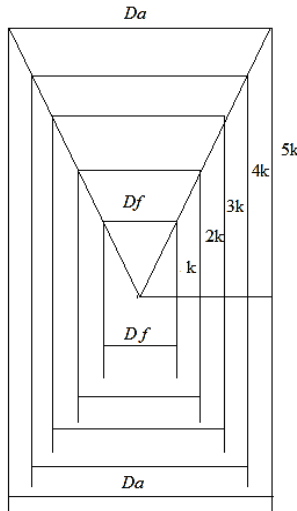


Figure 4 Formed triangles

The PWM switching voltages producing current signals are shown for inductive loads (L) in the PWMs in Fig. 5.

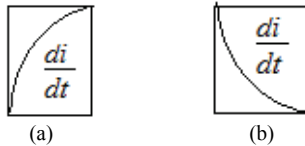


Figure 5 (a) PWM producing current in between $T/2$ and T , (b) PWM producing current in between 0 and $T/2$

The size changes of the SSPWMs are $1a, 2a, 3a, 4a, 5a$ in the period of $T/2$ as shown in Fig. 6.

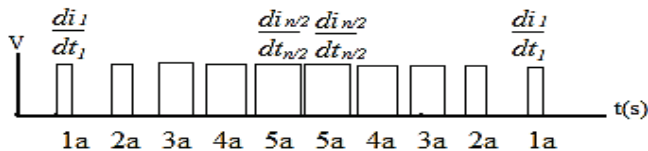


Figure 6 A linear increases of the PWM signals is created in the comparison of the results

While controlling switch, the step sinus pulse width modulation provides the total current for the inductive load (L) in Fig. 6 as in the Eq. (16).

$$\frac{di}{dt} = L \cdot \left(\frac{di_1}{dt_1} + \frac{di_2}{dt_2} + \dots + \frac{di_{n/2}}{dt_{n/2}} + \frac{di_{n/2}}{dt_{n/2}} + \dots + \frac{di_2}{dt_2} + \frac{di_1}{dt_1} \right) = 2L \sum_{k=1}^{n/2} \frac{di_k}{dt_k} \quad (16)$$

If two triangles are used to produce SSPWM for every step in the horizontal size of the steps which are increased for $2b$, two same SSPWMs are created on every step as in Fig. 7.

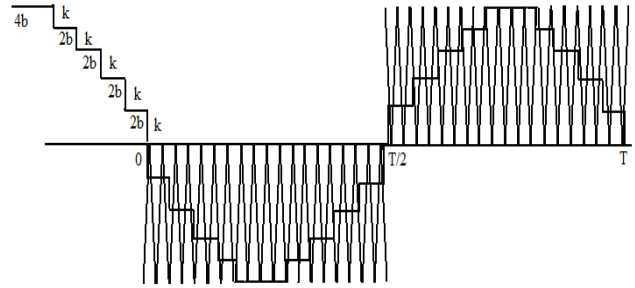


Figure 7 A linear increases of the angular PWM signals is created in comparison of the results

The width changes for the SSPWMs are $2 \times (1a, 2a, 3a, 4a, 5a)$ in the period of $T/2$ as shown in Fig. 8.

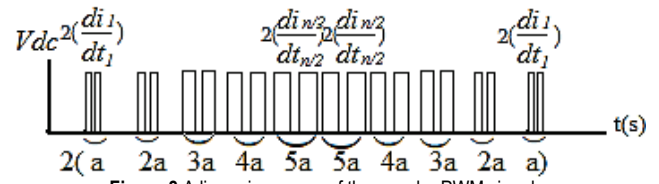


Figure 8 A linear increases of the angular PWM signals

The angular step sinus pulse width modulation produces the total current of the equation in Fig. 6 as in the Eq. (17) for inductive loads.

$$\frac{di}{dt} = 2L \cdot \left(\frac{di_1}{dt_1} + \frac{di_2}{dt_2} + \dots + \frac{di_{n/2}}{dt_{n/2}} + \frac{di_{n/2}}{dt_{n/2}} + \dots + \frac{di_2}{dt_2} + \frac{di_1}{dt_1} \right) = 4L \sum_{k=1}^{n/2} \frac{di_k}{dt_k} \quad (17)$$

The switching times create a total alternating voltage according to the step sinus pulse width modulation on a period of $T/2$. The switch times increase from D_f to D_a . The increases are linear because of the similar triangle rules because comparison of steps and triangles are arranged for creating triangular similarity as in Fig. 4. There are n pulses in a period of $T/2$. Therefore, the pulses are added as Eq. (18).

$$\left(\frac{D_f + D_a}{2} \right) \cdot n \quad (18)$$

4 DC MOTOR DESIGN

The DC motor's mathematical model implements a separately created DC machine. The model has certain parameters. The resistance of armature is R_a in ohms and the inductance of armature is L_a in henries. The resistance of field is R_f in ohms and the inductance of field is L_f in henries. The field armature's mutual inductance is L_{af} in henries. The total inertia of the DC machine is J in $\text{kg}\cdot\text{m}^2$. The total friction coefficient of the DC machine is B_m in $N\cdot\text{m}\cdot\text{s}$. The total Coulomb friction torque constant of the DC

machine is T_f in N·m. KE is the voltage constant and w is the machine speed in rad/s. The armature current is i_a in ampere. The field current is i_f in ampere, the electrical torque is T_e in Nm. The field terminal exists between (F+, F-) with the inductance L_a and resistance R_a in the series. The armature circuit is constructed between the A+ and A- which contain the inductance L_a and the resistance R_a in the series with a counter-electromotive force E calculated as the Eq. (19).

$$E = K_E w \tag{19}$$

E is proportional to the field current I_f in a separately created DC machine model and K_E is calculated as the Eq. (20)

$$E = L_{af} \dot{I}_f \tag{20}$$

The mechanical part is described as the Eq. (21).

$$J \frac{dw}{dt} = T_e - T_L - B_m w - T_f \tag{21}$$

The state space equation is formed for the machine speed w as the Eq. (23).

$$\frac{J}{B_m} \frac{dw}{dt} - w = T_e - T_L - T_f \tag{22}$$

$$\dot{w} = \frac{T_e - T_L - T_f}{Js - B_m} \tag{23}$$

The DC machine model of the Matlab Simulink is shown in Fig. 9 according to the created mathematical equations.

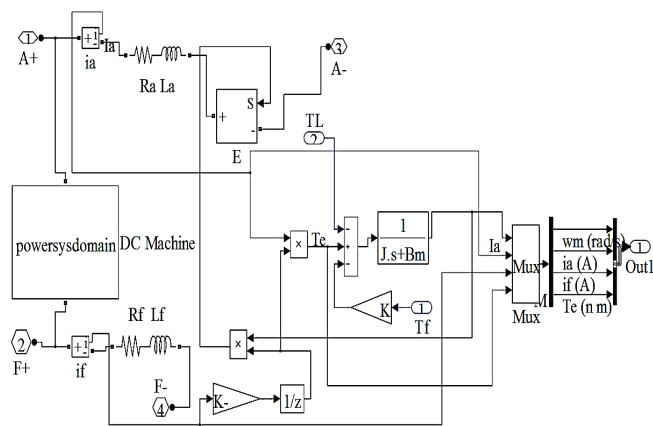


Figure 9 DC machine model of the Matlab Simulink

The DC machine model of the Matlab Simulink is given in Fig. 9 according to the created mathematical models. The PID control is considered to obtain a better result while running the system. The differential form of the PID controller is in the Eq. (24). The Laplace form of the PID

controller is in the Eq. (25). K_p is the proportional gain. K_i is the integral gain. K_d is the derivational gain.

$$u(t) = K_p e(t) + K_i \int e(t) dt + K_d \frac{de}{dt} \tag{24}$$

$$K_p + \frac{K_i}{s} + K_d s = \frac{K_p s^2 + K_p s + K_i}{s} \tag{25}$$

If the proportional gain, integral gain and derivational gain are applied to the DC motor equation, the Eq. (26) and Eq. (27) are formed as follows:

$$\dot{w} = K_p + \frac{K_i}{s} + K_d s \frac{T_e - T_L - T_f}{Js - B_m} \tag{26}$$

$$\dot{w} = \frac{K_p (Js^2 - B_m s) + K_i (Js - B_m) + K_d s^2 (T_e - T_L - T_f)}{Js^2 - B_m s} \tag{27}$$

5 EXPERIMENTAL RESULTS

The applications of the PID controlling DC motor on the closed-loop control and the constant DC source feeding the DC motor on an open-loop control are performed in the Matlab Simulink. The armature of the DC motor with the constant DC source is worked with 520 V while the armature of the DC motor with DC-DC converter is performed with 150 V at the closed-loop control as shown in Fig. 10.

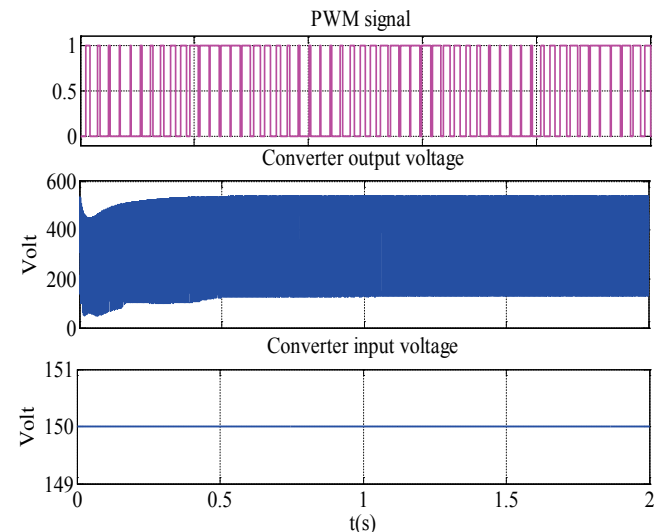


Figure 10 PID controlling the DC-DC converter of input, output voltages and the PWM signal

The speed of the DC motor which has 0.9 N·m of load can reach 115 rad/s (1100 rpm), while 240 V of the constant direct voltage source runs the DC motor as uncontrolled, which is an open-loop control as shown in Fig. 11. The speed of the DC motor which has 0.9 N·m of load reaches 145 rad/s (1385 rpm) on a closed-loop control, while 150 V of direct voltage feeding the converter runs the DC motor as

shown in Fig. 11. The PID controlling of the DC-DC converter achieves a high performance on the speed of the DC motor although the converter has low voltage according to the constant DC source.

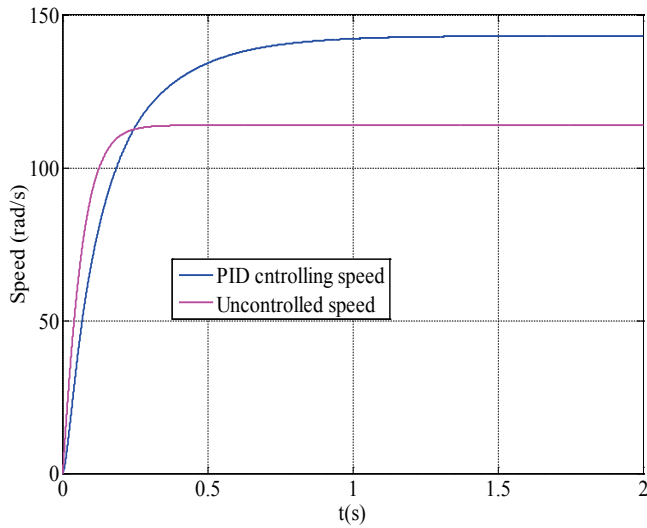


Figure 11 PID controlling the DC-DC boost converter and the constant DC source running the speed of the DC motors

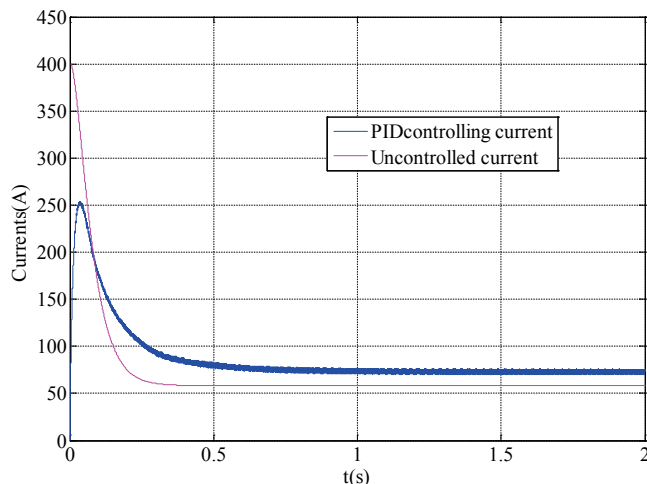


Figure 12 PID controlling the DC-DC boost converter and the constant DC source running the currents of the DC motors

After 240 V of the constant direct voltage running the DC motor as in an open loop control in Fig. 12, a settling current value of the DC motor can reach 62 A on 0.3 s while a starting current of the DC motor obtains a peak current value such as 400 A on 0.05 s. 150 V of the direct voltage feeding the power converter with, the DC motor runs on a closed-loop with a PID control. A settling current of the DC motor can reach 72 A on 0.1 s while the DC motor reaches 400 A of the peak current value on 0.5 s as in Fig. 12. Although the converter has a lower input voltage which is 150 V as opposed to the constant DC source of 240 V, the DC motor with the DC-DC converter achieves a high performance on a settling current of the DC motor in a closed-loop control.

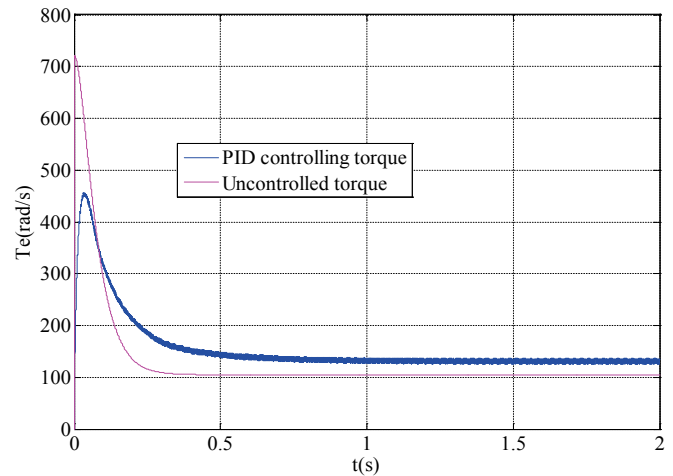


Figure 13 PID controlling DC-DC boost converter and a constant DC source running the torques of the DC motors

After 240 V of the constant direct voltage source runs the DC motor on open-loop control in Fig. 13, a settling torque of the DC motor can remain such as 105 Nm on 0.05 s while the maximum starting torque reaching 720 N·m on 0.3 s. When the 150 V of direct voltage feeding the DC-DC boost converter runs the DC motor with the PID controlling as in Fig. 13, a settling torque of the DC motor can reach 143 N·m on 0.1 s after 450 N·m of the maximum starting torque. The PID controlling DC-DC converter achieves high performance on the settling torque of the DC motor even though the input of the converter has a low input voltage according to the constant DC source which is 240 V.

The values of the used parameters are shown in Tab. 1 for the system constructed.

Table 1 Values of the used parameters

Parameter	Values	Parameter	Values
L_{af}	1.8 H	Converter input V_{dc}	150 V
L_a	0.012 H	L	0.1 mH
R_a	0.6 Ω	C	0.001 mF
R_f	240 Ω	K_p	0.002
L_f	120 H	K_i	0.001
B_m	0.2 N·m·s	K_d	0.001
J	0.5 km ²	TL	0.9 N·m
T_s	0.0001 s	Converter output V_{dc}	550 V

6 CONCLUSION

The DC motor and the DC-DC boost converter mathematical model were formed so that the PID controlling converter connecting the DC motor could be constructed at the Matlab Simulink. The PID controlling DC-DC boost converter driving the DC motor and a constant DC source driving the DC motor are simulated in the Matlab Simulink for the comparison of output performances after the formed mathematical model. The results are analyzed in this study after the system is performed. for the current and torque and speed of the DC motor, the DC motor which has a PID controlling DC-DC boost converter does a better performance on a closed-loop than a constant DC source

running the DC motor on an open-loop according to the results.

7 REFERENCES

- [1] Sen, P. C. *Thyristorised dc drives*. // Wiley Eastern Ltd 1979
- [2] Thadiappan, K.; Bellamkonda, R. A fast-response DC motorspeed control system. // IEEE Transactions on Industry Applications, vol. IA-10, no. 5, September/October 1974, pp. 843-851.
- [3] Sheel, S.; Chandkishore, R.; Gupta, O. Speed control of DC drive using MRAC technique. // International Conference on Mechanical and Electrical Technology, 10-12 September, 2010, Singapore, pp. 135-139
- [4] Borage, M.; Tiwari, S.; Bhardwaj, S.; Kotaiah, S. A full-bridge dc-dc converter with zero-voltage-switching over the entire conversion range. // IEEE Trans Power Electron. 2008 Jul; 23(4):1743-1750.
- [5] Wai, R. J.; Lin, C.Y.; Duan, R. Y.; Chang, Y. R. High efficiency DC-DC converter with high voltage gain and reduced switch stress. // IEEE Trans Ind Electron. 2007; 54(1):354-364.
- [6] Mao, H.; Rahman, O. A.; Batarseh, I. Zero-voltage-switching dc-dc converters with synchronous rectifiers. // IEEE Trans Power Electron. 2008 Jan; 23(1):369-378.
- [7] Thammasiriroj, Y.; Warit, et al. Nonlinear Model Based Single-Loop Control of Interleaved Converters for a Hybrid Source System. // ECTI Transaction on Electrical Engineering, Electronics, and Communications 15.1 (2017): 19-31.
- [8] Ai, J.; Mingyao, L. Ultra-Large Gain Step-Up Coupled Inductor DC-DC Converter With Asymmetric Voltage Multiplier Network for a Sustainable Energy System. // IEEE Transactions on Power Electronics (2016).
- [9] Sheel, S.; Gupta, S. Advanced techniques of PID controller tuning—development of a toolbox. // First International conference on Control, Instrumentation and Mechatronics CIM '07 at Persada Johor, Malaysia.
- [10] Kha, N. B.; Ahn, K. K. Position control of Shape Memory Alloy actuators by using self-tuning Fuzzy PID controller. // First IEEE Conference on Industrial Electronics and Applications, 2006, Singapore, pp. 1-5.
- [11] Thadiappan, K.; Bellamkonda, R. A fast-response DC motorspeed control system. // IEEE Transactions on Industry Applications, vol. IA-10, no. 5, September/October 1974, pp. 843-851.
- [12] Guan, E. Y. et al. Fundamental modulation: Multi-pattern scheme with an entire range of modulation indices for multilevel cascaded converter. // Proc. IEEE Ind. Electron. Appl. Conf., 2006, pp. 1-6.
- [13] Williams, J. Narrow-band analyzer (Thesis or Dissertation style). // Ph.D. dissertation, Dept. Elect. Eng., Harvard Univ., Cambridge, MA, 1993.
- [14] Chiasson, J.; Tolbert, L. M.; McKenzie, K. J.; Du, Z. Control of a multilevel converter using resultant theory. // IEEE Trans. Control Syst. Technol., vol. 11, no. 3, pp. 345-354, May 2003.
- [15] Wilkinson, J. P. Nonlinear resonant circuit devices (Patent style), U. S. Patent 3 624 12, July 16, 1990.
- [16] Kerem, A.; Aksoz, A.; Saygin, A.; Yilmaz, E. N. Smart grid integration of micro hybrid power system using 6-switched 3-level inverter. // In Smart Grid and Cities Congress and Fair (ICSG), 2017 5th International Istanbul (pp. 161-165). IEEE.
- [17] Can, E.; Sayan, H. H. PID and fuzzy controlling three phase asynchronous machine by low level DC source three phase inverter/PID i neizravno upravljanje trofaznim asinhronim motorom pomocu trofaznog izmjenjivaca slabe istosmjernje struje. // Tehnicki vjesnik-Technical Gazette, 23, 3(2016): 753-761.
- [18] Can, E.; Sayan, H. H. SSPWM three phase inverter design and experimented on unbalanced loads. // Tehnicki vjesnik-Technical Gazette, 23, 5(2016): 1239-1244.
- [19] Saygin, A.; Aksoz, A.; Yilmaz, E. N. A different model of WECS connected to smart grid through matrix converter. // In Smart Grid Congress and Fair (ICSG), 2016 4th International Istanbul (pp. 1-5). IEEE. (2016, April).
- [20] Can, E.; Sayan, H. H. Different Mathematical Model for the Chopper Circuit. // Tehnicki glasnik-Technical Journal, (2016), 10(1-2), 13-15.
- [21] Can, E.; Sayan, H. H. The increasing harmonic effects of SSPWM multilevel inverter controlling load currents investigated on modulation index. // Tehnicki vjesnik-Technical Gazette, 24, 2(2017). <https://doi.org/10.17559/TV-2015102013462>

Authors' contacts:

Dr. Erol CAN, Assistant Professor

Department of Aircraft Airframe Powerplants,
School of Civil Aviation, Erzincan University, Erzincan, Turkey
E-mail: can_e@hotmail.com

Dr. H. Hüseyin SAYAN, Associate Professor

Department of Electrical and Electronics Engineering,
Faculty of Technology, Gazi University, Ankara, Turkey
E-mail: hsayan@gazi.edu.tr